The United Nations University

GEOTHERMAL TRAINING PROGRAMME
Orkustofnun, Grensásvegur 9,
IS-108 Reykjavík, Iceland

Reports 2006
Number 12

THE CHEMISTRY OF GEOTHERMAL WATERS OF SW-UGANDA

Dan Mainza
Ministry of Energy and Mineral Development
Department of Geological Survey and Mines
Plot 21-29 Johnstone Road
P.O.Box 9, Entebbe
UGANDA
danielmainza@yahoo.co.uk

ABSTRACT

The SW-Uganda geothermal areas are located outside the active volcanic zones of the western arm of the East African Rift Valley with varying proximity. In this study, the Cl-SO_4-HCO_3, Li-Cl-B, and Na-K-Mg ternary diagrams, stable isotopes, silica and cation geothermometers, mixing models and saturation index plots were used to characterize the waters and estimate the subsurface temperature. The results show that most of the waters are in partial equilibrium with the rock but seem to be associated with volcanism. Waters of Ihimbo, Kitagata, and Rubaare are partially equilibrated; Kisiizi, Kagamba and Bubare are immature waters while the rest plot on the boundary between partially equilibrated and immature. It follows then, that the geoindictors can be applied to Ihimbo, Kitagata, and Rubaare with a fairly good degree of confidence. The geothermal waters from Kagamba, Birara, Bubare and Kisiizi are peripheral or mixed with cold groundwater while Rubaare, Ihimbo, Kanyinabarongo, and Kitagata waters are probably volcanic. The rest may be a combination of the two. The waters are meteoric and of local origin, with no apparent $\delta^{18}O$ shift. This may indicate that hydrothermal alteration reactions have long ceased; aquifer temperatures are not high; and good permeability exists.

From the plausible geothermometers the predicted subsurface temperatures are: 50-60°C for Kisiizi; 50-80°C for Kagamba, Bubare and Kanyinabarongo; 80-100°C for Kiruruma and Ihimbo; 100-120°C for Karungu; 100-130°C for Kitagata, Rubabo 1 and 2, and Minera; and 100-140°C for Rubaare. The SiO_2 enthalpy model and solution- mineral equilibria also give a similar range of subsurface temperature predictions.

1. INTRODUCTION

This report is part of the course in Chemistry of Thermal Fluids that the author attended at the United Nations University Geothermal Training Programme (UNU-GTP) for six months from May to October 2006. The course gives insights into the role of thermal fluid chemistry in geothermal exploration and exploitation, including sampling, analysis of major constituents and the interpretation of results. Much emphasis is placed on the application of chemical geothermometers and the calculation of mixing models. Environmental aspects of the thermal fluids are also considered.

The study of the chemistry of geothermal fluid samples can yield information on a number of field characteristics, at a relatively low cost. As an aid to assessing the energy content of the field, the most important parameter estimate is the subsurface temperature, which cannot normally be obtained except by very costly drilling. Chemical analysis can also provide information on the type of system (e.g. vapour-dominated, hot water), the origin of the fluids, geology and mineralogy at depth, fluid-mixing processes, possible scaling and corrosion problems in any future development and zones of high vertical permeability, as well as the range of composition and the economic value (if any) of the constituents. Furthermore, regular monitoring of the composition of geothermal fluids constitutes an important tool in the assessment of environmental impacts.

Uganda is currently facing power shortages due to climatic fluctuations, with a shortfall in electricity supply at peak periods amounting to almost 200 MW, and this has brought about a slowdown in the economic growth of the country (Ministry of Finance, 2006). As a short term measure, the government has licensed Independent Power Producers (IPPs) to produce thermal power to overcome the shortfall. However, the high price of petroleum products is making the electricity price too high for sustainable economic development. Therefore, sustainable sources of energy are being sought and among these is geothermal energy. The geothermal energy resource in Uganda has been estimated at about 450 MWe (McNitt, 1982).

Exploration of natural hot water in Uganda dates back to 1930 when the Geological Survey made brief reconnaissance investigations of the geothermal resources. However, the oldest literature on the Ugandan geothermal systems dates way back to the late 19th Century when Stanley described the salt works at Lake Katwe crater, and measured the temperature of the lake and one of the hot springs in the crater to be 29.1 and 32.5°C, respectively (Stanley, 1890; Gíslason et al., 1994). In the recent past, exploration has focused on the Katwe, Kibiro and Buranga fields, with surface exploration in Kibiro and Katwe prospects completed and deep exploration about to commence.

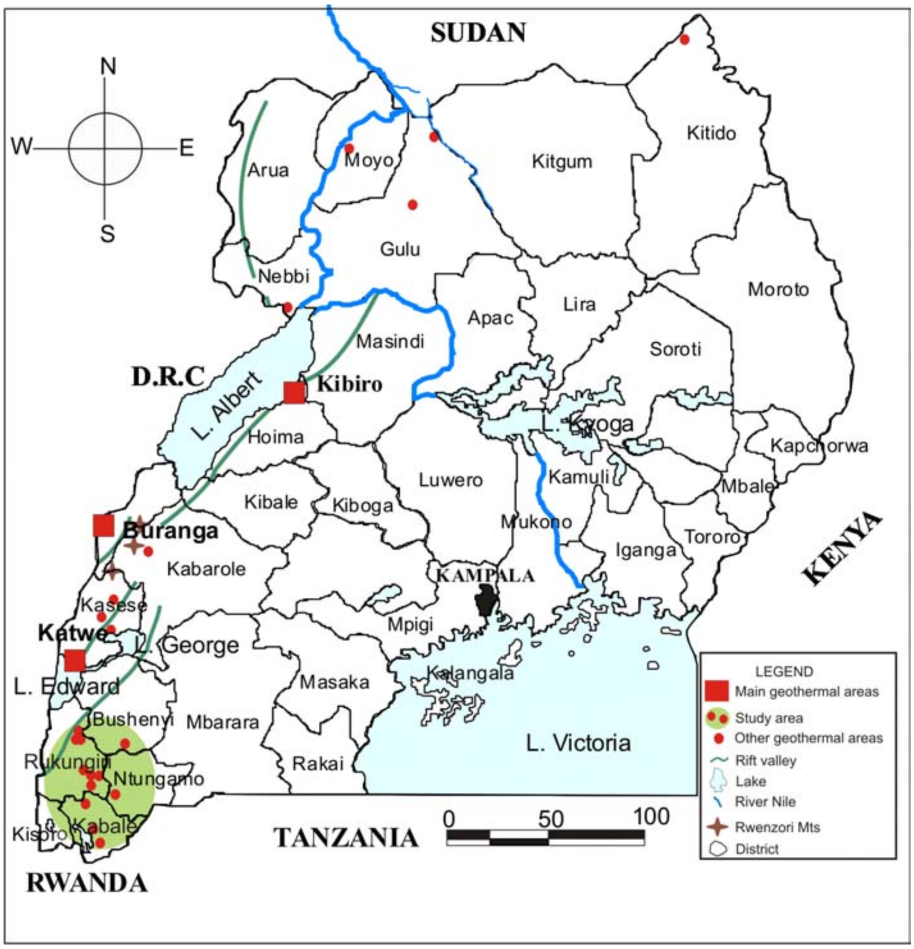

FIGURE 1: Locations of the geothermal areas in Uganda

Preliminary geothermal investigation of other areas of Uganda (Figure 1) involving geochemical, hydrological and geological surveys is being carried out with the aim of ranking the geothermal areas of Uganda in terms of their geothermal potential for more detailed surface analysis. This includes SW-Uganda which is the area under study in this report.

The author applied geochemical methods

to characterise geothermal fluilds and estimated the subsurface temperatures of the geothermal fields of SW-Uganda which lie outside the active volcanic belt.

2. BACKGROUND

2.1 Geological setting

The geology of Uganda (Figure 2) consists of an exposed pre-Cambrian basement bisected by the western branch of the East African Rift system in the western part of the country. The eastern branch, the Gregory Rift, passes through the central part of Kenya. The Western Rift starts to the north along the Sudan border, and then curves to the west and southwest along the border with the Democratic Republic of Congo, and south to Rwanda and Burundi. Rifting began at least 15 million years ago in Miocene time. The western rift is considered to be at an early stage in development, and is younger (Late Miocene – Recent) than the more mature eastern branch (Morley et al., 1999). The region of the rift has a markedly higher heat flow than the surrounding Pre-Cambrian terrain. Two different en echelon strands are found in the Western Rift, separated by the Rwenzori Mountains, which rise from a base of less than 1000 m in the Rift to over 5000 m elevation. Within the rift valley there are thick layers of late Tertiary and Quaternary sediments, fresh water and saline crater lakes, volcanics, and plutonic bodies have been identified beneath L. Albert and L. Edward (EDICON, 1984). The majority of geothermal areas of Uganda are found in the Western Rift Valley (Figure 1).

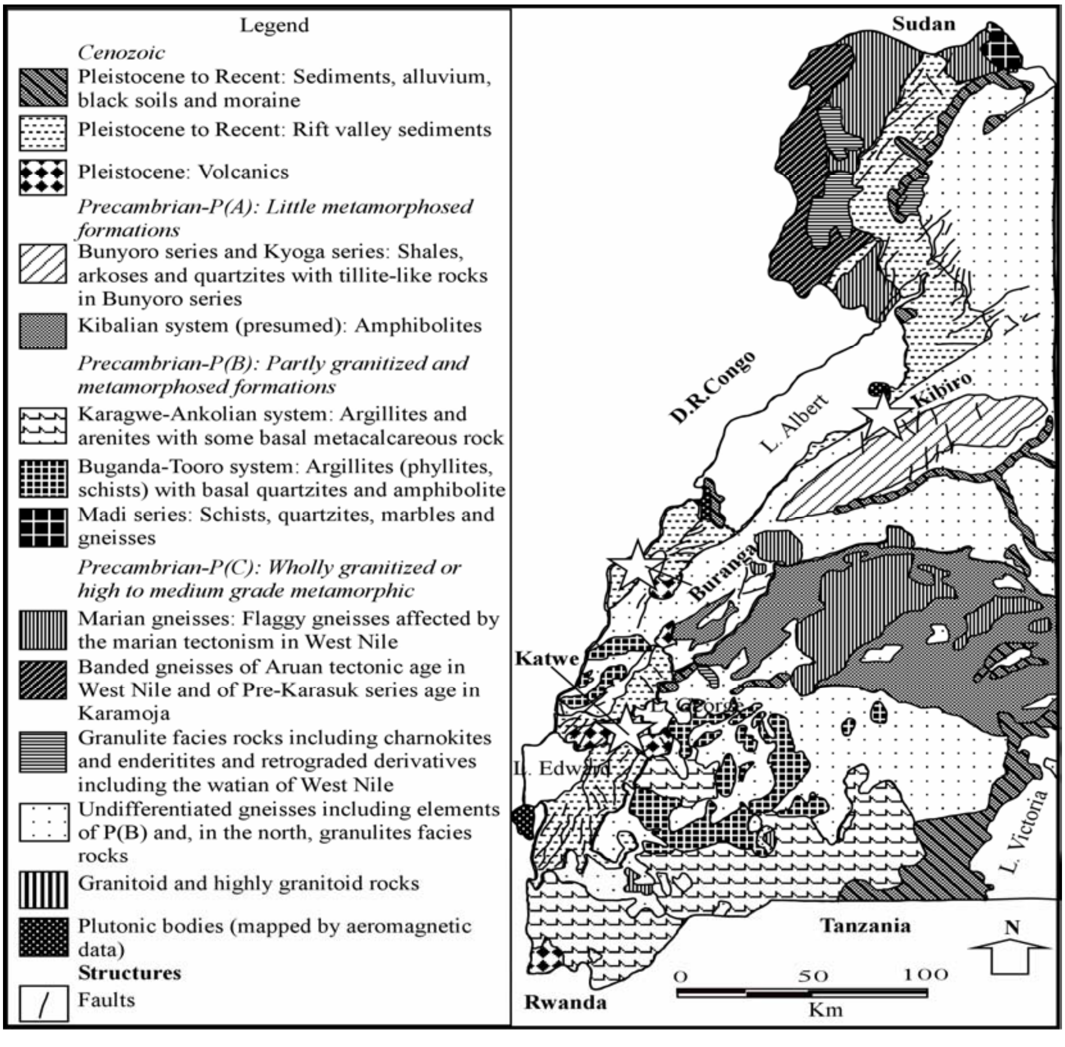

FIGURE 2: The geology of the Western Rift Valley in Uganda

2.2 Previous studies

Data and Bahati (2003) carried out preliminary geothermal investigations of the geothermal areas outside the active volcanic belt in SW-Uganda namely Rubabo, Minera, Ihimbo, Birara, Kiruruma, Rwagimba, Karungu, and Kitagata, all located on the outskirts or close to the Western Rift Valley in SW-Uganda. This investigation was carried out as a part of the recommendations of the *Geothermal Exploration project I* of 1993-1994. During the project, geological and geochemical investigations of the three areas Katwe-Kikorongo, Buranga and Kibiro were carried out. One of the recommendations of the project was that the hot springs outside the active volcanic belt be investigated and results compared with those from the active volcanic areas.

The geochemical results indicated that most of the geothermal waters from these areas are not in equilibrium with the rock although they seem to be associated with volcanism. The geothermal waters from Minera, Ihimbo and Kitagata do not appear to be mixed, with all the plausible geothermometers showing consistency. Subsurface temperatures of 100-130°C, 80-120°C and 120-140°C are predicted by geothermometry for Minera, Ihimbo and Kitagata, respectively.

The results (Table 1) for the geothermal waters from Birara, Karungu and Rubabo had two sets of geothermometer results and appear plausible. The two sets of geothermometer temperatures are possibly due to different reactions to cooling of the geothermal component by conduction or mixing with cold water in the upflow zone. In Birara, the NaK and NaKCa geothermometers yield temperatures in the range 145-160°C, but the quartz and KMg geothermometers yield 110-130°C. In Karungu, the NaK geothermometer gives 140-160°C while the quartz and KMg geothermometers give 90-110°C. In Rubabo, 110-115°C are obtained by the KMg and quartz geothermometers, but 125-140ºC with the NaK geothermometers.

TABLE 1: Earlier geothermometry results

Location	**Sample no.**	$T_{surface}$ **(°C)**	T_{quartz} **(°C)**	$T_{NaK\ 1}$ **(°C)**	$T_{NaK\ 2}$ **(°C)**	T_{NaKCa} **(°C)**	T_{KMg} **(°C)**
Karungu	UG-96-001	58.2	112.5	136	125.6	190.9	109.6
Kitagata	UG-96-006	58	126	157.7	146.3	155	110.7
Ihimbo	UG-96-009	36	81.9	85.4	75	171.8	127.7
Birara	UG-01-014	62	92.2	155.2	143.6	70.5	108.2
Rubabo	UG-01-015	56.5	94.5	124.7	116.2	103	121.4
Kiruruma	UG-01-016	70	116.5	88.3	80.1	257.3	
Minera	UG-01-017	69	121.5	136.6	128.1	76.4	226.8

T_{quartz}: Fournier and Potter, 1982; $T_{NaK\ 1}$: Arnórsson et al, 1982;
$T_{NaK\ 2}$: Truesdell and Fournier, 1977; T_{NaKCa}: Fournier and Truesdell, 1973;
T_{KMg}: Truesdell and Fournier, 1977.

In Kiruruma the subsurface temperature range of 80-100°C was inferred from geothermometry. The geothermometry temperatures are not consistent for this area, an indication that the fluids are not in equilibrium with the parent rock.

All the geothermal areas possess typical fluid temperatures for direct application of geothermal energy, i.e. for domestic use, agriculture and industrial heating. Most of the areas, i.e. Birara, Karungu Rubabo, Minera, Ihimbo and Kitagata, could provide fluids for binary turbine production of electricity. Some of the waters in these areas, with low total dissolved solids content, could be used as mineral water.

3. METHODOLOGY

3.1 Geochemical data collection

3.1.1 Sampling

Analytical results are only as good as the sampling and analytical techniques. It is imperative that the personnel involved in the sampling and chemical analysis of geothermal samples have an insight into the possible errors and interferences. The most common mistakes made during sampling are using improper containers, improper cleaning and the lack of or improper treatment for sample preservation. It is important that sample collection be properly carried out because all subsequent steps including chemical analysis depend on it. In the field it is important to keep a complete record of samples collected and a description of the sample locations. A copy of an outline of a field record card is shown in Appendix I. Some constituents will not survive intact from sampling to analysis without special precautions. Common reasons for concentration changes are interaction with suspended matter, adsorption on container walls, biological activity, redox reactions, polymerisation and precipitation. Different preservation methods are needed for the various processes and thus the total sample will comprise several sub-samples. Preservation methods may be physical or chemical; the most commonly used are listed in Appendix II.

The collection of samples can be divided into two categories, samples from natural springs, and hot water wells. When collecting samples from hot springs it is desirable that the water be free-flowing from the sampling spot, if not, a sampling pump is needed. A funnel connected to rubber tubing is submerged into the water to be sampled. The samples have to be cooled to ambient temperatures before being collected by connecting the tubing to a stainless steel cooling coil placed in a coolant like cold water. An example of a collection set up is shown in Appendix III. An untreated sample is collected for pH, carbonate, H_2S and conductivity measurements. If the SiO_2 concentration is greater than 100 ppm, the sample has to be diluted with distilled deionised water to an ideal concentration of 30-100 ppm into triplicates and the dilution factor recorded. A filtered sample (Fu) is collected for anions and a filtered and acidified sample (Fa) for cations. In cases of high sulphide concentrations, the sulphide is precipitated with Zn $(CH_3COO)_2$ and SO_4 analysed for. For the analysis of stable isotopes (δ^2H, $\delta^{18}O$) 60 ml of filtered samples are needed. The various sub-samples collected are described in detail in Table 2.

TABLE 2: Treatment and sub-samples from hot springs and hot-water wells

Treatment	Container	Specification	To determine
None; amber glass bottle with ground glass stopper	250-300 ml glass	Ru	pH, CO_2, H_2S (if not in field), conductivity
None	200 ml plastic	Ru	Mg, SiO_2 if < 100 ppm
Dilution; 50 ml of sample added to 50 ml of distilled, deionised water	3x100 ml plastic	Rd (1:1)	SiO_2 if > 100 ppm
Filtration	200 ml plastic	Fu	Anions
Filtration; 0.8 ml conc. HNO_3 (Suprapur) added to 200 ml sample	200 ml plastic	Fu	Cations
Filtration; 2 ml 0.2 M $ZnAc_2$ added to sample in 100 ml volumetric glass flask and ≥ 10 ml to ≥ 500 ml bottle containing ≥ 25 mg SO_4 to precipitate sulphide	100 ml, > 500 ml plastic	Fp; Fpi	SO_4,
Filtration; 160 ml and 2 1000 ml amber glass bottles	60 ml, 1000 ml gl	Fui, Fuc, Fut	^2H, ^{18}O, ^3H, ^{13}C

Fp - Filtered, precipitated;	Fpi – Filtered, precipitated for ^{34}S and ^{18}O in SO_4;
Fu - Filtered, untreated spectroscopy;	Fuc- Filtered, untreated for ^{13}C;
Fui- Filtered, untreated for ^2H and ^{18}O in water;	Fut- Filtered, untreated for tritium;
Rd - Raw, diluted;	Ru - Raw, untreated.

3.1.2 Chemical analysis and results

Analysis of water samples for pH, conductivity, total carbonate and H_2S was carried out in the field, and for the rest of the constituents in the Wairakei analytical laboratory, New Zealand. The analytical methods used are listed in Table 3.

TABLE 3: Analytical methods

Analyte	Method	Detection limit
B	ICP-OES APHA 3120-B 20th edition 1998	0.1 mg/l
K	ICP-OES APHA 3120-B 20th edition 1998	0.01 mg/l
Na	ICP-OES APHA 3120-B 20th edition 1998	0.01 mg/l
Li	ICP-OES APHA 3120-B 20th edition 1998	0.05 mg/l
Ca	ICP-OES APHA 3120-B 20th edition 1998	0.05 mg/l
Mg	ICP-OES APHA 3120-B 20th edition 1998	0.01 mg/l
Al	ICP-OES APHA 3120-B 20th edition 1998	0.1 mg/l
Fe	ICP-OES APHA 3120-B 20th edition 1998	0.02 mg/l
SiO_2	ICP-OES APHA 3120-B 20th edition 1998	0.5 mg/l
CO_2	Titration with 0.1 N HCl using a pH-meter	1.0 mg/l
SO_4	Ion Chromatography APHA 4110-B 20th edition	0.03 mg/l
Cl	Potentiometric APHA 4500-Cl-D 20th edition	20 mg/l
F	Ion Chromatography APHA 4110-B 20th edition	0.01 mg/l
H_2S	Titration with mercuric acetate and dithizone as indicator	0.04 mg/l
NH_3	ISE APHA 4500-NH_3-D 20th edition 1998	0.1mg/l
pH	pH-meter with a glass electrode	-
Conductivity	Conductivity meter	-
TDS	Conductivity meter	-
δ^2H	IR-MS (Donnelly et al., 2001)	± 0.5‰
$\delta^{18}O$	IR-MS (Epstein and Mayeda, 1953)	± 0.1‰

APHA: American Public Health Association (Clesceri et al., 1998)

The analytical results are presented in Table 4. All the samples are geothermal and were collected in 2005.

3.2 Origin of the geothermal fluids

By using isotopic techniques, Craig (1961) proved that the meteoric origin of geothermal waters can be determined by measuring the hydrogen and oxygen isotopic compositions of steam and water from geothermal fields; the isotopic ratio (R) is the number of atoms between a given isotope and the most abundant isotope of that element.

The deuterium ratio is found to be constant and the same as that of the local meteoric waters of the area, while the oxygen-18 concentration may show a characteristic enrichment which is known as "oxygen shift", meaning the shift of the isotopic composition towards an $^{18}O/^{16}O$ ratio higher than that of the local meteoric water.

The shift is due to isotopic exchange with the minerals forming the rock matrix through which the waters have moved. The meteoric waters infiltrating at depth to form a geothermal reservoir are in isotopic disequilibrium with the rocks, and exchange their oxygen with the surrounding rocks that are much richer in heavy isotopes in order to reach equilibrium corresponding to the temperature of the reservoir. The extent of the exchange depends on the relative proportions of oxygen in water and rocks, initial ^{18}O ratio, the water-mineral fractionation factor, reaction time and the surface contact area. The ^{18}O enrichment of the water entails a corresponding depletion of ^{18}O from the affected rocks. The hydrogen ratio is not appreciably affected because of the small hydrogen content of the rocks (about 1%) compared to oxygen (50% in mass).

The determination of the absolute isotopic composition of a sample is extremely difficult, whereas measurements of differences in composition are relatively easy. Therefore, measurements are carried out as a comparison with a standard sample of known isotopic composition and the result is the deviation per mil – delta (δ) – the enrichment of the heavier isotopes (depletion negative) relative to *Standard Mean Ocean Water*, SMOW (Árnason, 1976).

A linear relationship between δD and $\delta^{18}O$ for most cold water of meteoric origin has been observed. Friedman (1953) first discovered the covariance between δD and $\delta^{18}O$ values of natural water, comparing his hydrogen isotope data with the oxygen isotope data of Epstein and Mayeda (1953). Craig (1961) published many analyses of both isotopic ratios carried out on the same samples and defined the now universally recognised '*World meteoric line*' abbreviated as WML with the expression below:

$$\delta D = 8(\delta^{18}O) + 10$$

The above expression describes the global meteoric water line, and in spite of the complex interactions that occur during the meteoric process, there is a remarkably good worldwide correlation. However, some local meteoric lines have been defined. In the present study, the *Kenyan rain line*, defined by Clarke et al. (1990) with the following expression, was applied:

$$\delta D = 5.56(\delta^{18}O) + 2.04$$

Ármannsson (1994) defined another line, called the *Continental African rain line* (CARL) defined by the expression:

$$\delta D = 7(\delta^{18}O) + 11$$

TABLE 4: Analytical results; concentration in (mg/kg) and (‰) for stable isotopes

Location	Sample no.	Eastings	Northings	Elevat. (m)	Temp. (°C)	Cond. (µS)	pH	CO_2	H_2S	TDS	Al	NH_3	B	Ca	Cl	F	Fe	Li	Mg	K	SiO_2	Na	SO_4	^{18}O	D
Kagamba	UG-05-15	833389	9853726	1811	35	467	7.49	186	0	234	<0.1	0.13	0.3	29	<20	1.8	<0.02	<0.05	44	4.7	26	13.2	37	-4.9	-17.1
Karungu	UG-05-16	819757	9881140	1832	65	846	7.09	111	0	423	<0.1	<0.1	0.44	29	44	5.4	0.9	0.38	3.8	9.4	49	149	206	-3.97	-9.6
Bubare	UG-05-17	829628	9863762	1820	34	578	6.29	406	0	288	<0.1	0.1	0.27	60	<20	0.69	1.8	0.23	38	5.7	19.2	61	73	-3.93	-9.1
Rubaare	UG-05-18	175226	9901026	1380	54	1600	7.52	85	0	800	<0.1	0.48	0.78	70	177	6.0	0.08	0.29	1.4	14.9	106	285	417	-4.2	-12.1
Kitagata	UG-05-19	183938	9924709	1495	66	1110	7.92	56	0	552	<0.1	0.41	0.61	36	55	7.4	0.05	0.5	0.28	10.7	76	203	346	-3.3	-3.1
Ihimbo	UG-05-20	813593	9924179	1028	70	893	9.2	45	0.92	444	0.26	0.58	0.27	3.8	71	6.0	0.08	<0.05	0.02	5.6	66	186	219	-3.45	-4.1
Kanyinabarongo	UG-05-21	810489	9928818	999	38	992	7.37	58	0	492	0.12	0.63	0.66	31	92	2.6	6.8	0.05	4.5	9.0	34	173	280	-3.45	-5
Birara	UG-05-22	820887	9901717	1285	63	1072	7.44	647	0	536	<0.1	0.25	0.33	70	80	6.2	0.25	0.21	10.5	13.6	103	210	208	-3.51	-7.2
Rubabo1	UG-05-23	827785	9900154	1316	58	1069	7.14	230	0	532	<0.1	0.19	0.27	41	93	3.9	0.04	0.09	8.3	11.2	81	216	184	-3.61	-8.5
Rubabo2	UG-05-24	827934	9900287	1306	60	1077	7.5	235	0	537	<0.1	0.25	0.26	41	90	3.9	0.09	0.09	8.3	11.3	80	216	183	-3.58	-7.2
Kiruruma	UG-05-25	805752	9926349	994	36	609	7.09	124	0	304	0.22	0.95	0.34	36	22	2.7	0.4	0.08	2.9	9.4	57	110	182	-3.28	-4.7
Kisiizi	UG-05-26	827673	9889841	1666	30.1	292	7.43	106	0	144	<0.1	0.15	<0.10	30	<20	0.18	0.04	<0.05	18.9	3.8	17.5	5.8	14.7	-3.69	-7.9
Minera	UG-05-27	167309	9899970	1345	58	2180	6.88	547	0	1080	<0.1	0.21	0.65	70	181	2.5	0.23	0.7	22	23	83	482	361	-4.13	-10.7

3.3 Classification of geothermal fluids

3.3.1 Cl-Li-B diagram

The alkali metal probably least affected by secondary processes is Li. It may, therefore be used as a "tracer" for the initial deep rock dissolution process and as a reference to evaluate the possible origin of two important "conservative" constituents of geothermal water. Once added, Li remains largely in solution. The B content of thermal fluids is likely to reflect to some degree the maturity of a geothermal system; because of its volatility, it is expelled during the early heating up stages. Therefore, fluids from older hydrothermal systems can be expected to be depleted in B while the converse holds for younger hydrothermal systems. It is, however, striking that both Cl and B are added to the Li containing solutions in proportions close to those in crustal rocks. At high temperature Cl occurs largely as HCl and B as H_3BO_3. Both are volatile and able to be mobilized by high temperature steam. They are, therefore, quite likely to have been introduced with magmatic vapour invoked above to lead to the formation of the deep acid brine responsible for rock dissolution. At lower temperatures the acidity of HCl increases rapidly, and it is soon converted by the rock to the less volatile NaCl; B remains in its volatile form to be carried in the vapour phase even at lower temperatures. The Cl/B ratio is often used to indicate a common reservoir source for the waters. However, some caution is required in applying this interpretation, since waters from the same reservoir can show differences in this ratio, due to changes in lithology at depth over a field (e.g. the introduction of a sedimentary horizon), or by the absorption of B into clays during lateral flow. The position of a data point in such a triangular or trilinear plot is simply obtained by first forming the sum S of the concentrations C_i (in mg/kg) of all three constituents involved:

$$S = C_{Cl} + C_{Li} + C_{B/4}$$

From the sum (S), the percentages of C_{Cl} and $C_{B/4}$ are obtained, then D = B/4 % + 0.5 Cl % is computed. The Cl % and D are plotted as Y and X axes, respectively.

3.3.2 Cl-SO_4-HCO_3 diagram

Most geochemical techniques may with confidence be applied only to specified types of fluids with limited ranges of composition. Any such interpretation of geothermal water samples, therefore, is best carried out on the basis of an initial classification. The Cl-SO_4-HCO_3 ternary diagram is one of the diagrams for the classification of natural waters (Giggenbach, 1991). The position of a data point in such a triangular plot like above is obtained by first evaluating the sum S of the concentrations C_i (in mg/kg) of all three constituents involved:

$$S = C_{Cl}+C_{SO4}+C_{HCO3}$$

From the sum (S), the percentages of Cl and HCO_3 are obtained, then D = HCO_3 % +0.5Cl % is computed. The Cl % and D are plotted as Y and X axes, respectively.

In this diagram, composition ranges are indicated for several typical groups of water such as volcanic and steam-heated waters, mature waters and peripheral waters. Normally, the group best suited for the application of geoindicators comprises the neutral, low-sulphate, high-chloride 'geothermal' waters along the Cl-HCO_3 axis, close to the Cl corner, namely mature waters. In addition, not only can it be used to weed out unsuitable waters, but may provide an initial indication of mixing relationships or geographic groupings. For instance, the degree of separation between data points for high-chloride and bicarbonate waters gives an idea of the relative degree of interaction of CO_2 charged fluids at lower temperature, and of the HCO_3 contents increasing with time and distance travelled underground (Giggenbach, 1988). Thus, it is important to classify the samples into different groups to control the relationships of these samples in general, before further chemical studies.

The triangular Cl-SO_4-HCO_3 diagram can be used to classify the geothermal waters especially and to weed out unsuitable waters for geochemical techniques (Giggenbach, 1988).

3.3.3 Na-K-Mg diagram

Giggenbach (1988) pioneered techniques for the derivation of Na-K-Mg-Ca geoindicators. If only Na-K-Mg are considered, a triangular diagram can be used to distinguish between equilibrated, partially equilibrated (including mixed) and immature waters. Geothermometers can only be applied to the equilibrated and partially equilibrated waters. The triangular diagram is based on the temperature dependence of the two reactions:

$$K\text{-}feldspar + Na^{+} = Na\text{-}feldspar + K^{+}$$
$$2.8\ K\text{-}feldspar + 1.6\ water + Mg^{2+} = 0.8\ K\text{-}mica + 0.2\ chlorite + 5.4\ silica + 2\ K^{+}$$

The position of a data point in the triangular plot is first used to obtain the sum S of the concentrations C_i (in mg/kg) of all three constituents involved, as in the previous case; only individual constituents are manipulated differently.

$$S = C_{Na}/1000 + C_k/100 + \sqrt{C_{Mg}}$$

From the sum (S), $C_{Na}/1000$ % and $\sqrt{C_{Mg}}$ % are obtained, then D = $\sqrt{C_{Mg}}$ % + $0.5C_{Na}/1000$ % is computed. The Na % and D are plotted as Y and X axes, respectively.

The area of partial equilibrium suggests either a mineral that has dissolved but has not attained equilibrium, or a water mixture that has reached equilibrium (e.g. geothermal water) with dilute unequilibrated water (e.g. cold groundwater). Points close to the $\sqrt{Mg}$ corner usually suggest a high proportion of relatively cold groundwater, not necessarily "immature".

3.4 Geothermometers

Geothermometers or geochemical thermometers are used to estimate the subsurface temperature of geothermal reservoirs. There are mainly three categories: solute, gas and isotope geothermometers. For this report, water (solute) geothermometers are used and are described below. Solute geothermometers may be broadly classified into two groups: (1) those which are based on temperature-dependent variations in solubility of individual minerals; and (2) those which are based on temperature-dependent ion-exchange reactions which fix ratios of certain dissolved constituents (Fournier, 1991).

3.4.1 Silica geothermometers

Silica geothermometers are based on temperature-dependent variations in the solubility of silica species. The silica content of water from a hot spring or a well can be correlated with the last temperature of equilibration. Solubility of silica is dependent on pressure, temperature and salinity. However at temperatures below 300°C, and at depth generally attained by commercial drilling for geothermal resources, variations in pressure at hydrostatic conditions have little effect on the solubility of quartz and amorphous silica (Fournier and Potter, 1982; Fournier and Rowe, 1966), and added salt has a significant effect only at concentrations above about 2-3 wt% (Fournier, 1985). Above 300°C, small changes in pressure and added salt are important.

Quartz geothermometers work best for waters in the subsurface temperature range of 120-250°C (Arnórsson et al., 1983a; Arnórsson, 2000). At higher temperatures silica is likely to be deposited during the water's ascent. At lower temperatures other silica species such as chalcedony, cristobalite, or amorphous silica may control dissolved silica (Fournier and Rowe, 1966; Fournier, 1973; Arnórsson, 1975).

Fournier (1991) deals with the ambiguity in the use of silica geothermometers at temperatures below 180°C as chalcedony appears to control dissolved silica in some places and quartz in others. Chalcedony is a very fine-grained variety of quartz, probably not a separate mineral but a mixture of quartz and moganite and, with time, it probably all changes to quartz (Gíslason et al., 1997). Temperature, time and fluid composition all affect different crystalline forms of silica. Thus, in some places (old systems), where water has been in contact with rock at a given temperature for a relatively long time, quartz may control dissolved silica at temperatures down to 100°C. In other places (young systems), chalcedony may control dissolved silica at temperatures as high as 180°C.

The basic reaction for the dissolution of silica minerals is:

$$SiO_2\,(s) + 2H_2O = H_4SiO_4\,(aq)$$

When using quartz geothermometers, some factors should be considered (Fournier and Potter, 1982):

a) The temperature range in which the equations are valid;
b) Possible polymerization or precipitation of silica before sample collection;
c) Possible polymerization of silica after sample collection;
d) Control of aqueous silica by solids other than quartz;
e) The effect of pH upon quartz solubility;
f) Possible dilutions of hot water with cold water before the thermal waters reach the surface.

Equations relating the solubility, S (mg SiO_2 / kg water) to temperature in the range 20-250°C for various pure silica minerals are presented in Table 5:

TABLE 5: Temperature equations for Silica geothermometers; S is concentration of SiO_2 in mg/kg

Geothermometers	Equations
β Cristobalite (Fournier, 1977)	$t°C = \frac{781}{4.51 - \log S} - 273.15$
α Cristobalite (Fournier, 1977)	$t°C = \frac{1000}{4.78 - \log S} - 273.15$
Chalcedony (Arnórsson et al., 1983a)	$t°C = \frac{1112}{4.91 - \log S} - 273.15$
Quartz (no steam loss) (Fournier, 1977)	$t°C = \frac{1309}{5.19 - \log S} - 273.15$
Quartz (after steam loss at 100°C) (Fournier, 1977)	$t°C = \frac{1522}{5.75 - \log S} - 273.15$

3.4.2 Cation geothermometers

Cation geothermometers are based upon the temperature dependence of ion exchange or partitioning of alkalis between solutions and solid phases. The ratios of dissolved constituents change with changing temperature of equilibration. The following is the list of the geothermometers that were applied in this report.

TABLE 6: Cation geothermometers

Geothermometers	Equations
Na-K (Fournier, 1979)	$t°C = \dfrac{1217}{1.438 + \log(Na/K)} - 273.15$
Na-K (Truesdell, 1976)	$t°C = \dfrac{856}{0.857 + \log(Na/K)} - 273.15$
Na-K (Arnórsson et al., 1983a)	$t°C = \dfrac{933}{0.993 + \log(Na/K)} - 273.15$
Na-K (Giggenbach, 1988)	$t°C = \dfrac{1390}{1.750 + \log(Na/K)} - 273.15$
K-Mg (Giggenbach, 1988)	$t°C = \dfrac{4410}{14.0 + \log(K^2/Mg)} - 273.15$

The above equations give good results for many high-temperature geothermal waters. Anomalous temperatures have been found for waters high in calcium and of lower temperature.

Fournier and Truesdell (1973) proposed the empirical Na-K-Ca geothermometer which considered the participation of calcium in the aluminosilicates reaction

$$t°C = \frac{1647}{\log(Na/K) + \beta \log(\sqrt{Ca}/Na) + 2.24} - 273.15$$

where $\beta = 4/3$ for $Ca^{1/2}/Na > 1$ and $t < 100°C$;
$\beta = 1/3$ for $Ca^{1/2}/Na < 1$ or if $t_{4/3} > 100°C$

The mineralogical background of the geothermometer must not be forgotten. It is not correct to apply the Na/K or the Na-K-Ca geothermometers to acid waters, which would not be in equilibrium with feldspars, nor are they applicable to water systems in rocks with unusually high or low concentrations of a particular alkali unless direct correlations with measured temperatures are available.

3.5 Solution-mineral equilibrium

Geothermometers have been developed to predict reservoir temperature. However, various geothermometers can give different values for the temperature of a reservoir. This may be due to different reaction rates, or mixing with cold water in the upflow. Reed and Spycher (1984) have suggested that the best estimate of reservoir temperature can be attained by considering simultaneously the state of equilibrium between specific constituents in water and many hydrothermal minerals as a function of temperature. Therefore, if a group of minerals converges to equilibrium at a particular temperature, this temperature corresponds to the most likely reservoir temperature. The rising fluid has reacted chemically with rock.

The equilibrium state of minerals can be estimated by the ratio of the activity product (*Q*) to the equilibrium constant (*K*) over a range of temperatures. The equilibrium constant and the activity product are related to the Gibbs energy through:

$$\Delta Gr = -RT \ln K + RT \ln Q = RT \ln Q/K$$

where R = Gas constant;
T = Temperature (K).

The saturation index (SI) can be obtained from the solubility product and its activity product:

$$SI = \log Q - \log K = \log(Q / K)$$

All minerals in equilibrium at the same temperature converge to $SI = 0$; $SI < 0$ for an undersaturated solution, and $SI > 0$ for a supersaturated solution. If fluid mixes with dilute water, mineral curves will intersect at $SI < 0$, but if it has boiled at $SI > 0$. Aqueous speciation is calculated at several predetermined temperatures to obtain a log (Q_i / K_i) versus temperature relationships for each mineral for the water composition under consideration.

WATCH (Arnórsson and Bjarnason, 1993) and SOLVEQ (Reed and Spycher, 1989) are computer programs used to calculate the speciation of geothermal fluids. By reading chemical analyses of samples collected at the surface, they are used to compute the speciation and deposition potentials. Parameters obtained include the pH, the equilibrium constant (K), the activity products (Q), redox potentials, and partial pressures of gases for the given reaction at any given temperature.

3.6 Mixing models

The use of geothermometers to estimate subsurface temperatures from the composition of the surface discharges is based on the notion that geothermal fluids may cool in upflow zones either conductively or by boiling due to depressurization (adiabatic boiling), or through both processes. However, hot waters ascending from a geothermal reservoir may also cool by mixing in the upflow with shallow, relatively cold water. Mixing can bring about partial or complete chemical equilibration. If chemical equilibrium is established after mixing, the chemical geothermometers indicate the temperatures of the mixed water, not the hot component. Whether or not equilibrium is established after mixing, the temperature of the hot water cannot be established from a solubility relationship unless mixing is taken into account (Truesdell and Fournier, 1977). To be confident in any interpretation of mixing, groups of springs should be examined (rather than the chemistry of isolated discharges) and the results related back to the spatial (geographic) distribution of the springs (Arnórsson, 1985). Such mixing processes are often best illustrated by the use of mixing models.

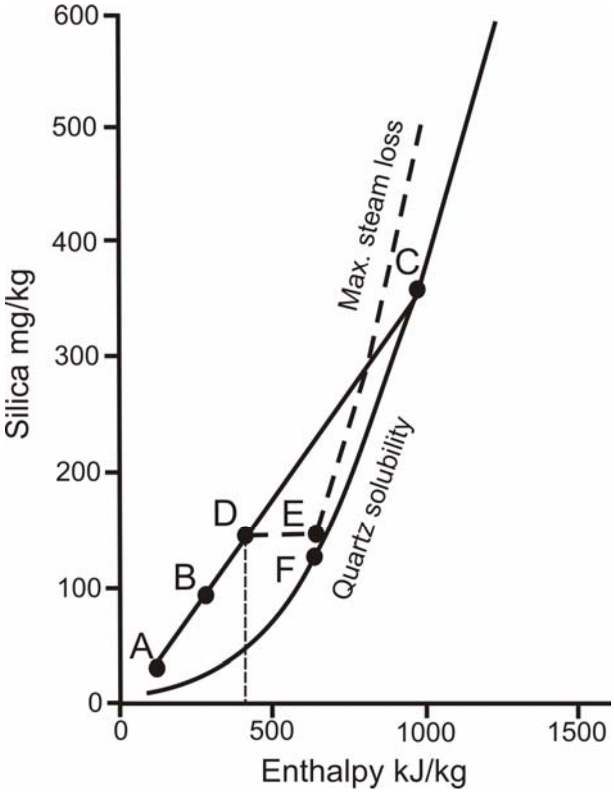

FIGURE 3: The silica enthalpy mixing model

The water in many hot springs consists of mixtures of deep hot water and shallow cold water. Truesdell and Fournier (1977) proposed a plot of dissolved silica versus the enthalpy of water to estimate the temperature of the deep hot water component. In this model, as illustrated in Figure 3, for a situation where no steam is lost before mixing, a straight line is drawn through A and B (representing a cold and a mixed-water warm spring, respectively) to intersect the quartz solubility curve at point C which gives the original silica content and enthalpy of the deep water. The original temperature of the hot-water component is obtained from steam tables. Enthalpy is used as a co-ordinate rather than temperature. This is because the combined heat contents of two waters at different temperatures are conserved when those waters are mixed, but the combined temperatures are not.

In a case where the maximum amount of steam is lost at atmospheric pressure prior to mixing, (point D, Figure 3), a horizontal line drawn from point D to intersect the maximum steam loss curve gives the initial enthalpy of the hot-water component (point E). The initial dissolved silica, prior to boiling and steam separation at atmospheric pressure, is shown by point F which lies directly below E. If the steam had been lost at a higher pressure before mixing, point D would lie above 419 kJ/kg (100°C) on the extension AB, and point E would lie between the maximum steam loss and quartz solubility curves.

There are some criteria for hot spring waters which may be appropriate for the application of this model: (1) a measured water temperature which is at least 50°C less than calculated silica and Na-K-Ca geothermometer temperatures, (2) a silica geothermometer temperature which is lower than the Na-K-Ca temperature, (3) a mass flowrate which is high enough to allow for only a little conductive cooling. This model cannot be applied to boiling springs because heat is carried away in the steam after mixing (Fournier, 1991). It is also assumed that no silica deposition takes place before or after mixing and that quartz controls the solubility of silica in hot water.

4. STUDY AREAS

Kagamba geothermal area is located on the Kabale – Katuna road approximately 10 km from the town of Kabale. Clear fresh water seeps under a pool of water. The area is swampy and characterized by clay soils of a wetland type which are generally representative of the lowlands of the Kabale district. The presence of moulds of travertine is evidence for a system that was thermally active in the past and has since cooled down. No outcrop was seen but floats of ferruginised phyllites / slates and quartzite were noticed. Just about 50 m across the road, ferruginised quartzite is quarried for aggregates. A fault is inferred in the area striking in a north-south direction and possibly controlling the hot springs. Water issues at about 35°C with intermittent gas bubbling. The flowrate is estimated at 0.1 l/s. This flow has formed a pool of water, 30 m x 10 m in size.

Karungu geothermal area is located in Hamurwa Subcounty, Rubanda County in Kabale district. The thermal area is situated south of the Kerere Forest Reserve, which is at a distance of approximately 35 km from the town of Kabale along the Kabale-Kanungu road. The geothermal area can easily be accessed by road through Nyamasiizi on the Kabale-Kisoro road. There are about 12 hot springs in the area which issue from the bed of the Ishasha river (trending E-W) from two sets of very narrow cracks, one coinciding with the bedding plane and the other with a joint plane, which runs at an angle to the bedding plane.

The area is underlain by hard ferruginised Karagwe-Ankolean phyllites / slates, jointed and bedded (trending north and dipping east). Some joints are nearly vertical. A faulted plane is inferred along the river Ishasha gorge. The hot water issues at a temperature between 34.4 and 65°C. Intermittent gas bubbling was observed in almost all the hot springs. The nearest volcano is at Kitunga with lava flows some 30 km away along the Kabale – Kisoro road. The hot spring water is used by locals for bathing, watering animals and as a tourist attraction.

Bubare geothermal area is located on the Kabale-Kisoro road approximately 4.8 km from Kabale. The area is underlain by ferruginous phyllites and slates of the Karagwe-Ankolean system. The geothermal water issues at a temperature of 34°C. Intermittent gas bubbling was noticed in a pool of warm water, 10 m x 5 m in size. At a distance of 150 m is another warm spring that has created a pool of water, 1 m in diameter, with a temperature of 28°C. Samples were collected from the first pool whose flowrate is 1.7 l/s.

Rubaare geothermal area is located in Rugarama sub-county, Rushenyi County in Ntungamo District. There are two hot springs, one of which has formed a pool, about 15 m diameter, and the second is located 100 m from the first; it is a small pool, 2 m in diameter. Some sort of structural control is inferred. The water was clear, and inactive fossil travertine (older spring deposits) was noted at high elevation within a radius of 200 m from the hot spring. The springs have thus been active at a higher elevation than today. The current extent of travertine appears disproportionately large relative to the current rate of spring overflow. Water issues from fractured quartz-rich pegmatite granitoid rock, with muscovite sheets and tourmaline. The presence of algae is more highly pronounced in the smaller pool than the bigger one possibly because a limited surface area is exposed. Surface water temperature was 54°C in both springs and the flow from the bigger pool about 2 l/s.

Kitagata geothermal area is located in Kitagata subcounty, Igara County, Bushenyi district. It is situated on the Ishaka-Kabale road at a distance of approximately 16 km from the town of Ishaka and 0.8 km from Kitagata trading centre. The thermal area is characterized by a number of hot springs issuing from banded fractured biotitic granitic gneiss, which is jointed (four sets) in the broad Rwabanjari valley. There is a presence of gas bubbling which is a characteristic of nearly all the hot springs in SW-Uganda. The temperature of the water at the sampling point is 67°C. The total flowrate is 4.1 l/s.

Striations were noted on the gneiss, an indication of a possible fault in this area, trending approximately N-S. E-W foliation trends were observed and N-S almost vertical joints. A pool of water, 7 m x 10 min size, has been curved out for bathing and is fed by water from the hot springs. Some iron oxide mineralisation was observed. About 300 m away is another hot spring (Omugabe pool), discharging at 2.8 l/s. This also issues from granitic gneiss forming a pool, about 9 m in diameter. Again, intermittent gas bubbling was noticed. White oolitic spring deposits were noticed on the gneiss surface and along fracture planes. It reacted slowly with acid. The hot spring water is used by locals for bathing, watering animals and as a tourist attraction.

Ihimbo geothermal area is located in Bwambara subcounty, Rujumbura County, Rukungiri district. The geothermal area is situated in Ihimbo forest at a distance of about 1.5 km from the Rukungiri - Kihihi road via Bugangari, Bwambara and Nyamirama and about 2 km from River Ntungwa, River Birara being its main tributary. It is located on or close to the presumed major boundary step rift fault, at the escarpment front of the western Rift Valley. The springs issue from Tertiary rift sediments (conglomerates, clays, silts and sands). The grains and pebbles of quartz are rounded to sub angular and the beds appear to contain iron oxide deposited from infiltration solutions, which give the beds their rusty brown colour. The highest temperature of 70°C was measured in one of the springs with the highest flowrate of 3 l/s. There are three groups of springs with temperatures of 70°C, 50°C and 68°C all on a 150 m long line, an indication that the thermal area is large. These hot springs are aligned in an approximately N-S direction possibly related to the major rift. Intermittent gas bubbling was noticed.

The presence of travertine is on record (Sharma, 1971). The thermal waters are used by people from all walks of life for bathing and are believed to cure several diseases.

Kanyinabarongo warm spring is located in Bwambara's sub-county, Rujumbura County, in the Rukungiri district. The Kanyinabalongo thermal springs are located north but not far from Ihimbo and seem to be aligned in a north-south direction. They issue from a pebbly clay (Pleistocene sediments) environment in the Rift Valley. More warm springs are reported in the area but these were the most pronounced. The surface water temperature is 38°C with a flow of about 4 l/s. A pool, about 4 m in diameter, is used by locals for its therapeutic values.

Birara geothermal area is located in Buyanja's sub-county, Rubabo County, in the Rukungiri district. The area is situated on the banks of the River Birara gorge with the hot springs issuing fresh clear water with a lot of gas bubbling which may be mistaken for boiling in some of the springs. The River Birara gorge is likely to be a fault through mica schists grading into gneiss. These rocks look ferruginous in places and micaceous. The highest measured temperature is 63°C in one of the springs. At this site the River Birara passes between two ridges, about 800 m high, and the hot springs are believed to be fault controlled. Despite the difficult terrain, the hot spring water is used by locals for bathing, watering animals and as a tourist attraction.

Minera geothermal area is located in Buyanja subcounty, Rubabo County, in Rukungiri district. The area is situated on the banks of the River Birara at a distance of about 20 km on the Rukungiri-Kabale road via Kebisoni trading centre. Several points of fossil thermal features could be noticed around the hot springs including geothermal grass and salt gardens. It is about 25 km from the edge of the rift valley. Mineral hot springs issue clear water with moderate gas bubbling at some points. Gas seeps were noticed along the river at a distance of 20 m downstream. Water issues from fractured crystalline basement rocks (granitic gneiss rock, with quartzite bands of the Karagwe-Ankolean system) jointed with different sets. A flowrate of 0.5 l/s and a maximum temperature of 58°C in the main spring were recorded. The hot spring water is used by locals for bathing, watering animals and as a tourist attraction.

Rubabo geothermal area is located in the Nyarushanje subcounty, Rubabo County, in the Rukungiri district. This area is also situated on the banks of the River Birara at a distance of 10 km downstream from the Minera geothermal area and on the Rukungiri-Kabale road. The thermal area can be divided into two groups of hot springs, namely Rubabo 1 and Rubabo 2, both of which were sampled.

The hot springs issue from a fractured crystalline basement (jointed and fractured) granitic gneiss rock, along the deeply incised Minera river gorge, some 20 km from the rift valley. The temperature ranges from 58 to 60°C. The thermal water is clear and fresh with a flowrate of 3 l/s, and intermittent gas seeps from nearly vertical joint sets (N-S). Another joint set was recorded at 110°/60°SW. The flow is fracture controlled in crystalline basement rocks. In the neighbourhood there are limestone deposits in a swamp. The hot spring water is used by locals for bathing, watering animals and as a tourist attraction.

Kiruruma geothermal area is located in the Kihihi subcounty, Kinkizi County in Kanungu district. The geothermal area is situated at a distance of about 10 km on the Kihihi-Katunguru road and on the banks of the River Kiruruma. It issues from unconsolidated rift Pleistocene sediments (conglomerates, sands, silts and clays) at a distance of about 50 m from the river and has a low surface temperature with a maximum of 36°C. A number of warm springs issue clear fresh water, with intermittent gas bubbling. The sediments are ferruginised in some places manifested in observable rusty stains. Thermal springs are located at or near a fault plane. A flowrate of about 1 l/s was recorded. The hot spring water is used by locals for bathing, watering animals and as a tourist attraction.

Kisiizi warm spring is located in the Nyarushanje subcounty, Rubabo County in the Rukungiri district. The thermal area is situated close to Kisiizi hospital along the Kabale – Rukungiri road. Kisiizi thermal springs issue clear warm water of about 30°C. Fractured silicified quartzitic rocks and granitic gneisses of the Karagwe-Ankolean system, underlie the area. The geothermal springs are probably controlled by fractures with an average flow of about 0.5 l/s. The warm water is currently used by Kisiizi hospital for bathing and other domestic uses. This is the only direct application of geothermal heat in Uganda, except for bathing in primitive pools.

5. RESULTS

5.1 Origin of the geothermal fluids

All the points plot close to the African rain line as shown in Figure 4 implying that the waters are meteoric, with no apparent $\delta^{18}O$ shift which may be an indication that: hydrothermal alteration reactions have long ceased to take place; aquifer temperatures are not high; or good permeability exists. They plot further away from the World Meteoric line and Kenya rainline than the local rainline, an indication that the origin is local.

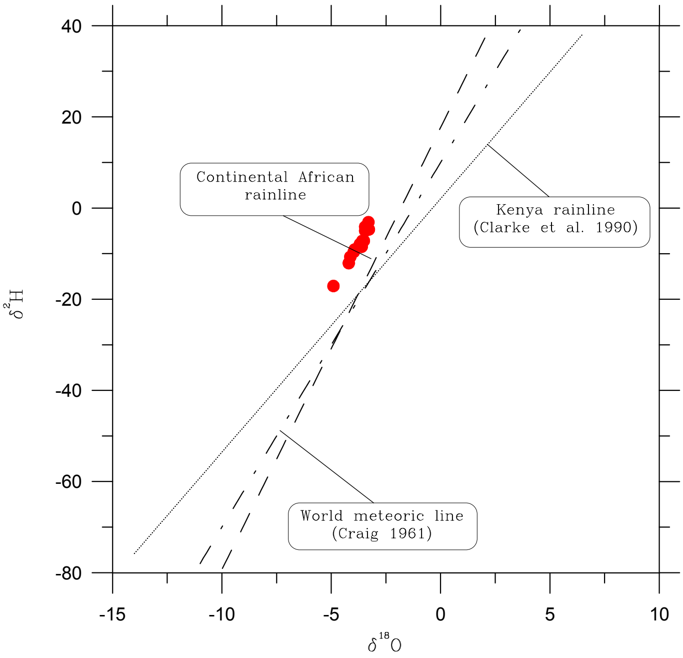

FIGURE 4: Stable isotope compositions of thermal waters from SW-Uganda

5.2 Classification of the fluids

Cl-SO$_4$-HCO$_3$ diagram. From Figure 5, it can be seen that the thermal waters from Kagamba, Birara, Bubare and Kisiizi have high HCO$_3$ relative to SO$_4$ and Cl suggesting that they are peripheral waters or having a high proportion of cold groundwater. Rubaare, Ihimbo, Kanyina-barongo, and Kitagata have a high SO$_4$ relative to HCO$_3$ and Cl, indicating that they may be volcanic waters. The other samples plot between peripheral and volcanic waters, which might be an indication that they are combined waters.

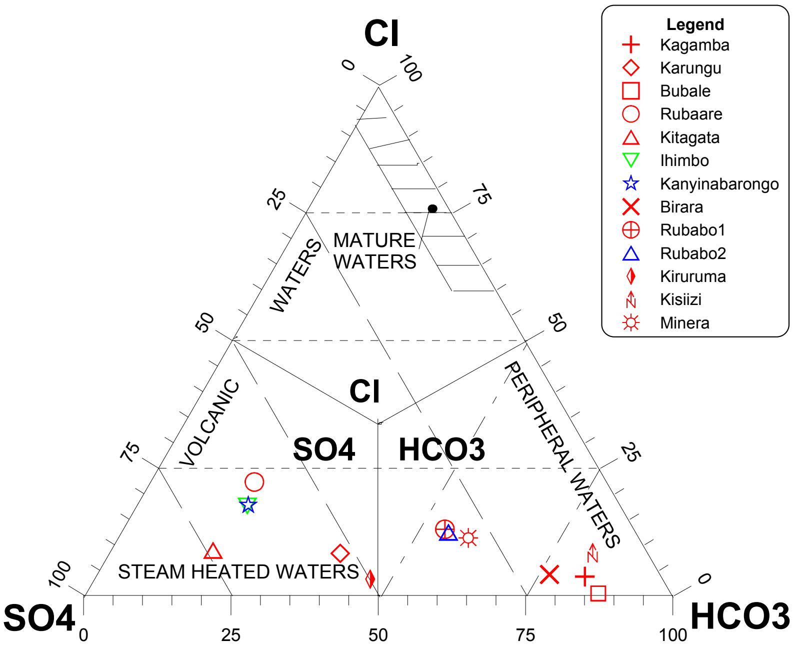

FIGURE 5: Classification of the thermal fluids using Cl-SO$_4$-HCO$_3$ diagram

Cl-Li-B diagram. Figure 6 shows that all the thermal water samples have a high Cl content, some very high relative to Li and B, indicating that they are from relatively old hydrothermal systems and the fluid migrates from the old basement rock. The exceptions are Karungu, Bubare and Kitagata which plot close to the base rock, indicating that perhaps they have not equilibrated.

Na-K-Mg diagram. As illustrated in Figure 7, Ihimbo, Kitagata, and Rubaare are partially equilibrated. Kisiizi, Kagamba and Bubare are immature waters or have a high proportion of cold groundwater, while the rest plot on the boundary between partially equilibrated and immature. The waters of Ihimbo, Kitagata, and Rubaare either have minerals that have dissolved but have not attained equilibrium, or the equilibrated waters have mixed with dilute unequilibrated water (e.g. cold groundwater). It follows that geoindictors can be applied to most of the waters with a fair degree of confidence except for Kisiizi, Kagamba and Bubare which plot close to the Mg corner.

5.3 Geothermometry

In Table 7, estimates by Na/K geothermometers for Kagamba, and Kisiizi are unrealistic, possibly because their $\sqrt{(M_{Ca})}/M_{Na}$ ratio is greater than 1, an indication that they have low subsurface temperatures as predicted by the quartz geothermometer (Fournier and Truesdell, 1973).

The anomalously high estimates of the Na-K-Ca geothermometer for all the samples could be due to calcium carbonate deposited during the ascent which prevents aqueous K and Na from interacting with the country rock (Fournier and Truesdell, 1973).

The quartz temperature function from Fournier and Potter (1982) is employed because the basement rock formations in SW-Uganda are of Pre-Cambrian age. The most important silica mineral in them and overlying sediments is quartz which is, therefore, the mineral controlling the silica concentration of the geothermal fluids. Thus, a quartz geothermometer is even applicable to temperatures below 150°C (Ármannsson, 1994).

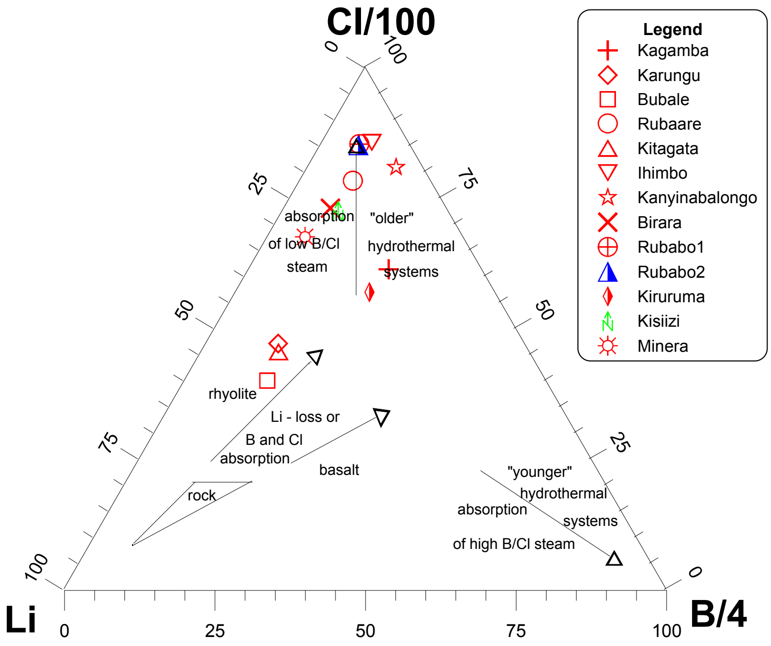

FIGURE 6: Classification of the thermal fluids using Cl-Li-B diagram

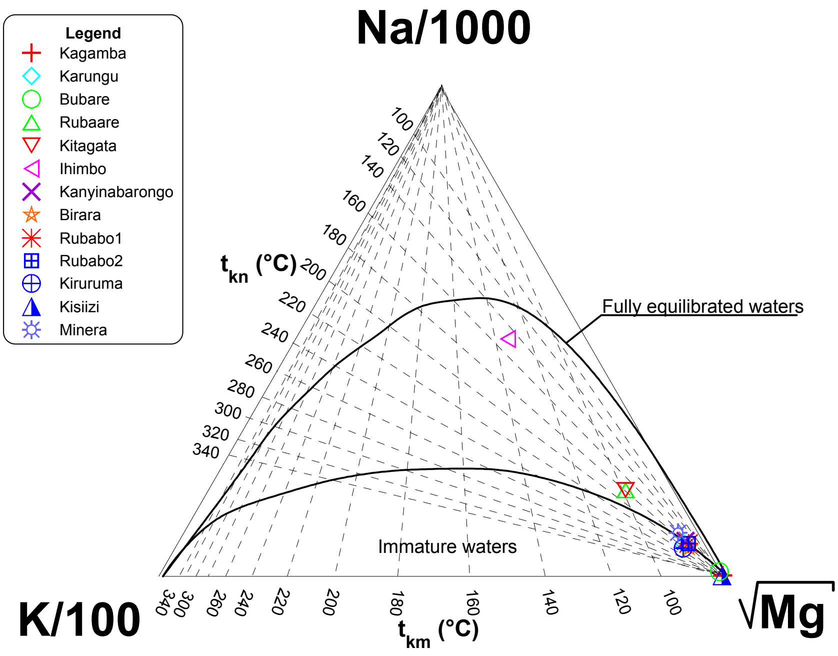

FIGURE 7: Classification of the thermal fluids using Na-K-Mg diagram

The geoindicators cannot be applied with full confidence to Kisiizi, Kagamba and Bubare because they plot close to the Mg corner. Further still, since the pH values of all the samples are less than 9.8, dissociation of silicic acid never arises (Arnórsson et al., 1983b). However, the Ihimbo sample, with a pH of 9.2, is susceptible to silicic acid dissociation although it is not likely to affect the geothermometer estimate greatly.

TABLE 7: Geothermometer results, temperatures in °C

Locations	Sample no.	$T_{Surface}$	T_{NaK}	T_{NaKCa}	T_{Quartz}
Kagamba	UG-05-15	35	338.9	234.9	73.3
Karungu	UG-05-16	65	153.9	179.0	100.6
Bubare	UG-05-17	34	194.7	177.6	62.0
Rubaare	UG-05-18	54	134.6	172.7	138.3
Kitagata	UG-05-19	66	136	173.0	119.6
Ihimbo	UG-05-20	70	95.8	162.0	90.0
Kanyinabarongo	UG-05-21	38	136.4	170.8	84.5
Birara	UG-05-22	63	155.9	178.7	135.9
Rubabo 1	UG-05-23	58	136.2	172.1	124.6
Rubabo 2	UG-05-24	60	137	172.6	122.9
Kiruruma	UG-05-25	36	183.9	188.1	107.6
Kisiizi	UG-05-26	30.1		258.4	58.1
Minera	UG-05-27	58	128.1	177.1	123.9

$T_{Surface}$: Surface temperature; T_{NaK} & T_{Quartz}: Watch, version 2.3/2004; T_{NaKCa} : Fournier and Truesdell, 1973.

5.4 Solution-mineral equilibria

The WATCH computer program is used to carry out aqueous speciation calculations for each sample. The results are used to plot a saturation index (SI) against temperature for the minerals present (Figure 8).

The data for Birara, Bubare, Rubabo 1, and Minera is unreliable because of the high ionic balances, -40.46%, 33.15%, 10.74% and 18.11%, respectively, and should be interpreted with caution.

From SI plots, it is clear that the samples have neither undergone boiling, which is to be expected for intermediate-enthalpy geothermal fields, nor mixing with cold groundwater since the points of convergence for the mineral plots is at SI = 0. This implies that the subsurface temperatures of the fields correspond to the point of convergence which is the point of equilibria for the minerals. The quartz temperature estimates (Table 7) lie within (or close to) the subsurface temperature range estimates (Table 8) from the plots in Figure 8.

TABLE 8: Quartz temperature estimates in °C

Location	T_{range} (°C)
Kagamba	40-50
Karungu	100-120
Bubare	60-70
Rubaare	120-130
Kitagata	120-130
Ihimbo	80-100
Kanyinabarongo	80-90
Birara	120-130
Rubabo 1	120-130
Rubabo 2	120-130
Kiruruma	80-100
Minera	80-100

T_{range}: Temperature

5.5 Mixing model

Figure 9 shows the silica enthalpy graph for the samples; the results are summarised in Table 9. The plot shows that the thermal waters of Rubaare, Kitagata, Ihimbo, Rubabo 1, Rubabo 2, Minera, Kiruruma and Birara are probably mixing with boiling, with Minera and Rubaare probably having a lot of boiling and mixing. However, the applicability of this model to the Minera waters is questionable since its flowrate 0.5 l/s, is too low (Fournier, 1991).

TABLE 9: Temperature estimates in °C

Locations	Sample no.	T_1 (°C)	T_2 (°C)
Rubaare	UG-05-18	>300	170
Kitagata	UG-05-19	200	150
Ihimbo	UG-05-20	160	140
Birara	UG-05-22	270	160
Rubabo1	UG-05-23	200	150
Rubabo2	UG-05-24	200	150
Kiruruma	UG-05-25	280	170
Minera	UG-05-27	200	150

T_1: No steam loss before mixing
T_2: Maximum steam loss before mixing

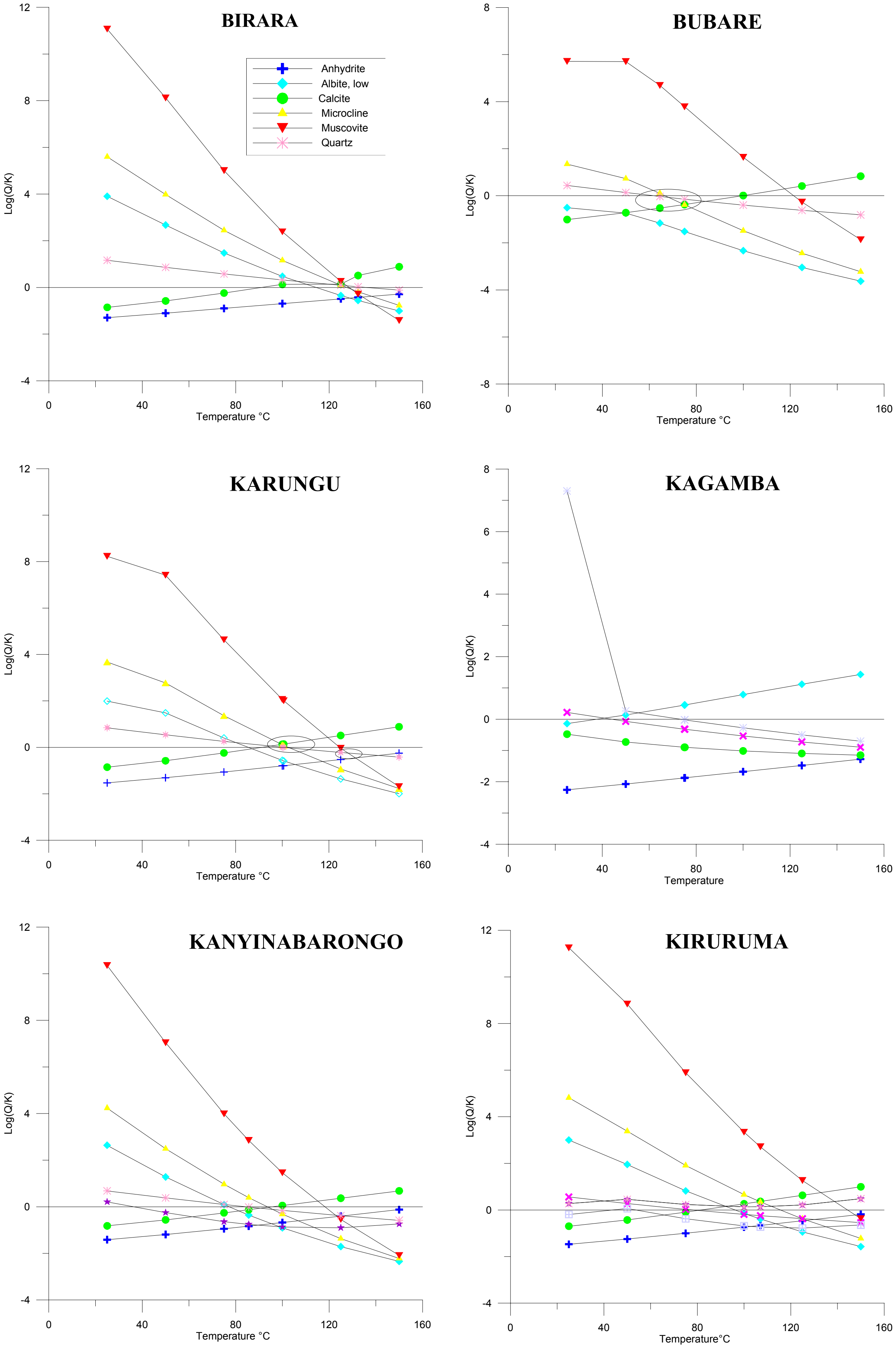

FIGURE 8: SI vs. temperature plots for waters from SW-Uganda

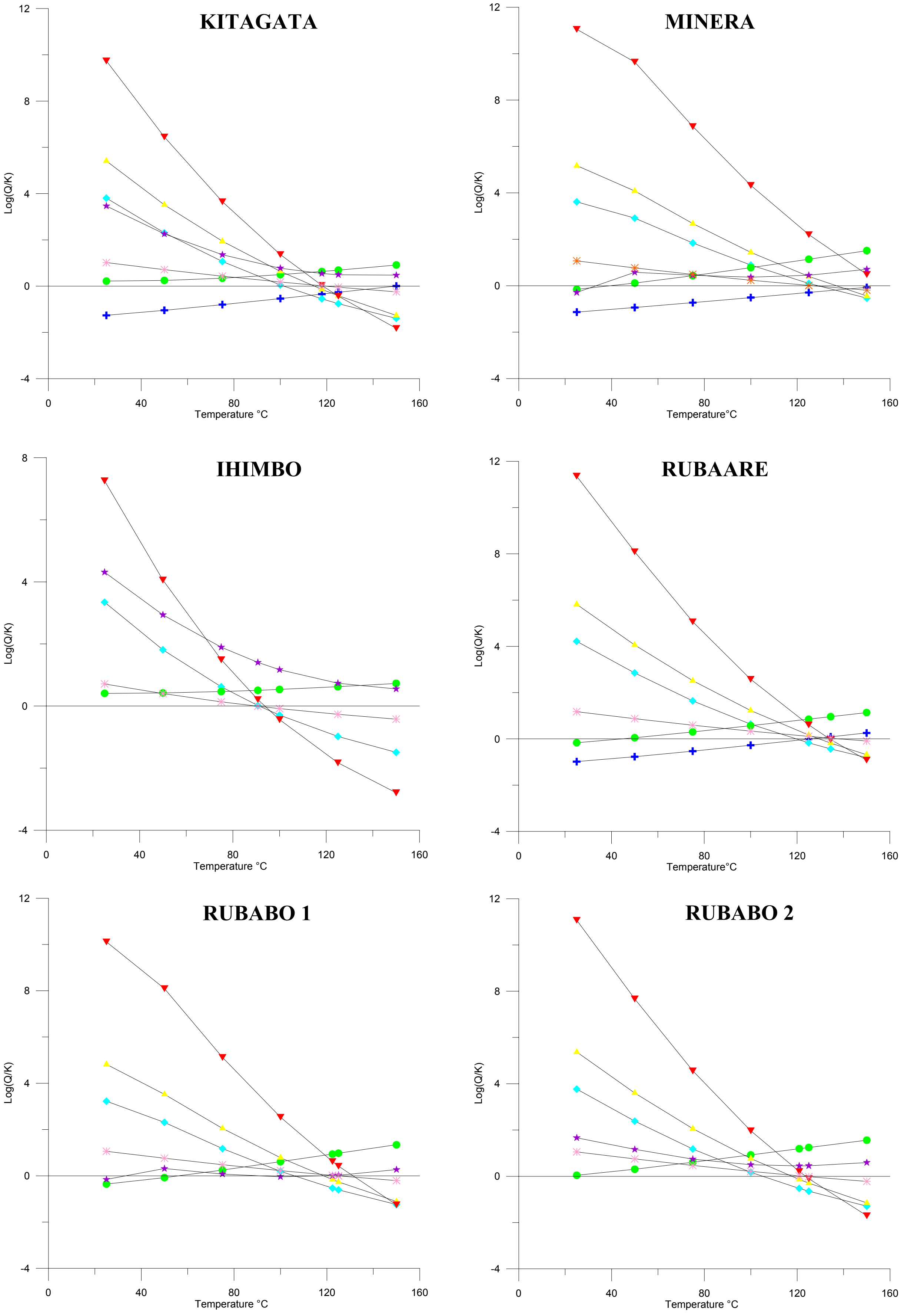

FIGURE 8 cont.: SI vs. temperature plots for waters from SW-Uganda

The high predictions for Birara are highly doubtful given the high values for CO_2 and Mg (Table 4), which suggest a low-temperature field. Arnórsson (1975) states that CO_2 rich waters tend to dissolve silicate minerals so rapidly that neither quartz nor chalcedony precipitation can cope with it for kinetic reasons; amorphous silica probably controls its dissolution.

Kagamba, Karungu, Bubare, Kanyinabarongo, and Kisiizi waters have a difference of less than 50°C between the measured and calculated quartz geothermometer temperatures; therefore, this model is not applicable (Fournier, 1991), further supporting the fact that they are just lukewarm waters.

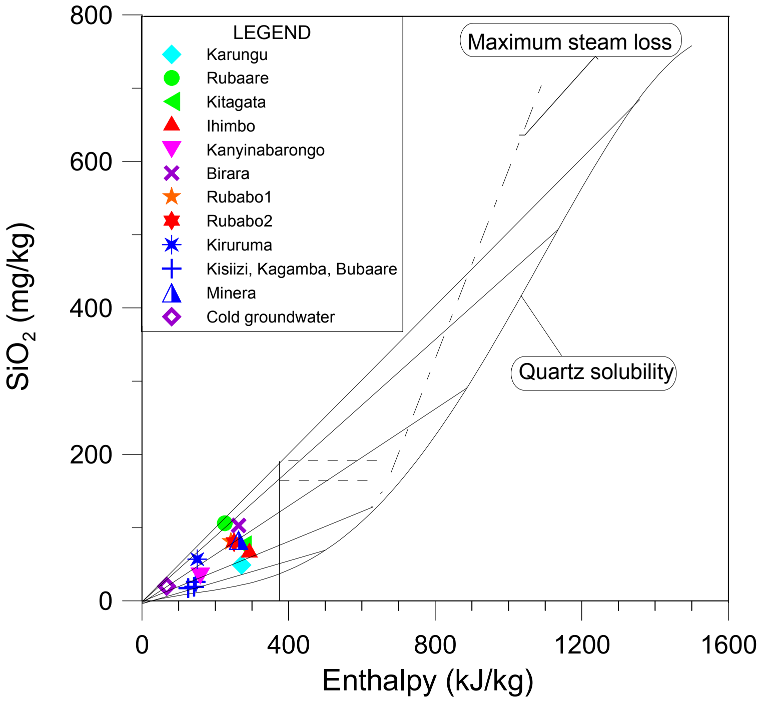

FIGURE 9: The use of silica enthalpy mixing model for the SW-Uganda waters

However, it must be noted that there was no cold groundwater sample available. Predicted values of 20 ppm SiO_2 and 20°C temperature were used, since in the study areas the concentration of SiO_2 in cold water should be about 20 ppm, given the average ambient temperature of about 20°C.

6. CONCLUSIONS

6.1 Main results

The main objectives of this project were to study the chemical characteristics of thermal fluids from SW-Uganda geothermal areas, determine the type and origin of the waters, and predict the subsurface temperature. The following conclusions were drawn:

- On the ternary plots,. Ihimbo, Kitagata, and Rubaare waters are partially equilibrated, Kisiizi, Kagamba and Bubare are immature waters, and the rest plot on the boundary between partially equilibrated and immature. The Ihimbo, Kitagata, and Rubaare waters could either have minerals that have dissolved and not reached equilibrium, or have been mixed with cold groundwater. However, geoindicators can still be applied with some good degree of confidence. The geothermal waters from Kagamba, Birara, Bubare and Kisiizi are probably peripheral; Rubaare, Ihimbo, Kanyinabarongo, and Kitagata are probably volcanic waters (SO_4 rich); the rest are a mixture of the two.
- All the waters suggest old hydrothermal systems.
- The waters are meteoric and of local origin, with no apparent $\delta^{18}O$ shift which may indicate that: hydrothermal alteration reactions have long ceased occurring; aquifer temperatures are not high; or good permeability exists.
- From the plausible geothermometers, the following summary of the predicated subsurface temperature in Table 10 is drawn:

TABLE 10: Summary of subsurface temperature predication in °C

Locations	Sample no.	Surface temperature	Predicated subsurface temperature
Kagamba	UG-05-15	35	60-80
Karungu	UG-05-16	65	100-120
Bubare	UG-05-17	34	60-70
Rubaare	UG-05-18	54	100-140
Kitagata	UG-05-19	66	100-130
Ihimbo	UG-05-20	70	70-120
Kanyinabarongo	UG-05-21	38	50-90
Birara	UG-05-22	63	110-140
Rubabo 1	UG-05-23	58	100-130
Rubabo 2	UG-05-24	60	100-130
Kiruruma	UG-05-25	36	80-100
Kisiizi	UG-05-26	30.1	50-60
Minera	UG-05-27	58	100-130

6.2 Recommendations

- Samples of cold groundwater from each area are needed for a detailed study on the fluid flow characteristics to enhance modelling of the geothermal system.
- From the predicted subsurface temperatures, Rubaare, Ihimbo, Rubabo, Birara and Kitagate can be used for generating electricity using a binary system. This is advantageous given the remote location of most of the areas from the national grid and the ever increasing demand for electricity.
- A study should be carried out to look into other possible areas of utilization such as: controlling humidity in greenhouses in order to enhance yields in horticulture; drying agricultural products; more in-house uses such as at Kisiizi hospital; and bottling the mineral waters, especially those with low TDS (total dissolved solids).

ACKNOWLEDGEMENTS

I would like to express my heartfelt gratitude to Dr. Ingvar B. Fridleifsson and Mr. Lúdvík S. Georgsson for giving me the opportunity to attend the UNU Geothermal Program, and for their moral support and help throughout the whole training period. I am indebted to Dr. Halldór Ármannsson, my advisor, for his assistance and critical advice during the preparation of this report. Special thanks go to all the lecturers for their comprehensive presentations and willingness to share their knowledge and experience. Mrs. Gudrún Bjarnadóttir and Ms. Thórhildur Ísberg deserve my thanks for the daily arrangements and help they rendered during the course.

I extend my appreciation to the Government of Uganda for allowing me to participate in this program.

REFERENCES

Ármannsson, H., 1994: *Geothermal studies on three geothermal areas in West and Southwest Uganda.*UNDESD, UNDP project UGA/92/002, report, 85 pp.

Árnason, B., 1976: *Groundwater systems in Iceland traced by deuterium.* Soc. Sci. Islandica, 42, Reykjavík, 236 pp.

Arnórsson, S., 1975: Application of the silica geothermometer in low-temperature hydrothermal areas in Iceland. *Am. J. Sci., 275,* 763-783.

Arnórsson, S., 1985: The use of mixing models and chemical geothermometers for estimating underground temperature in geothermal systems. *J. Volc. Geotherm. Res., 23,* 299-335.

Arnórsson, S. (ed.), 2000: *Isotopic and chemical techniques in geothermal exploration, development and use. Sampling methods, data handling, interpretation.* International Atomic Energy Agency, Vienna*,* 351 pp.

Arnórsson, S., and Bjarnason, J.Ö., 1993: *Icelandic Water Chemistry Group presents the chemical speciation programme WATCH.* Science Institute, University of Iceland, Orkustofnun, Reykjavík, 7 pp.

Arnórsson, S., Gunnlaugsson, E., and Svavarsson, H., 1983a: The chemistry of geothermal waters in Iceland III. Chemical geothermometry in geothermal investigations*. Geochim. Cosmochim. Acta, 47*, 567-577.

Arnórsson, S., Gunnlaugsson, E., and Svavarsson, H., 1983b: The chemistry of geothermal waters in Iceland II. Mineral equilibria and independent variables controlling water compositions. *Geochim. Cosmochim. Acta*, *47*, 547-566.

Arnórsson, S., Sigurdsson, S. and Svavarsson, H., 1982: The chemistry of geothermal waters in Iceland I. Calculation of aqueous speciation from 0°C to 370°C. *Geochim. Cosmochim. Acta, 46,* 1513-1532.

Clarke, M.C.G., Woodhall, D.G., Allen, D., and Darling, W.G., 1990: *Geological, volcanological and hydrogeological controls on the occurrence of geothermal activity in the area surrounding Lake Naivasha, Kenya.* Ministry of Energy, Nairobi, Kenya, report, 138 pp. + 3 maps.

Clesceri, L.S., Greenberg, A.E., and Eaton, A.D. (eds.), 1998: *Standard methods for the examination of water and wastewater* (20th edition). American Public Health Association, American Water Works Association and the Water Environment Federation, 1325 pp.

Craig, H., 1961: Isotopic variations in meteoric water. *Science, 133*, 1702-1703.

Data, G., and Bahati, G., 2003: The chemistry of geothermal waters from areas outside the active volcanic belt, SW-Uganda. *Proceedings of the 2nd Kenya Electricity Generating Co. Geothermal Conference, 2003, Nairobi, Kenya.*

Donnelly, T., Waldron, S., Tait, A., Dougans, J., and Bearhop. S., 2001: Hydrogen isotope analysis of natural abundance and deuterium- enriched waters by reduction over chromium on-line to a dynamic dual inlet isotope-ratio mass spectrometer. *Rapid Communications in Mass Spectrometry, 15-15,* 1297-1303.

EDICON, 1984: *Aeromagnetic interpretation of Lake Albert/Edward portion of the Western Rift Valley.* EDICON, Inc., Denver, Colorado, unpubl. report.

Epstein, S., and Mayeda, T.K., 1953: Variation of $\delta^{18}O$ content of waters from natural sources. *Geochim. Cosmochim. Acta, 4*, 213-224.

Fournier, R.O., 1973: Silica in thermal waters. Laboratory and field investigations. *Proceedings of the International Symposium on Hydrogeochemistry and Biochemistry, Tokyo, 1*, Clark Co., Washington D.C., 122-139.

Fournier, R.O., 1977: Chemical geothermometers and mixing model for geothermal systems.

Geothermics, 5, 41-50.

Fournier, R.O., 1979: A revised equation for Na-K geothermometer. *Geoth. Res. Council, Trans., 3,* 221-224.

Fournier, R.O., 1985: The behaviour of silica in hydrothermal solutions. *Rev. Econ. Geology, 2,* 45-61.

Fournier, R.O., 1991: Water geothermometers applied to geothermal energy. In: D'Amore, F. (coordinator), *Applications of Geochemistry in Geothermal Reservoir Development*. UNITAR/UNDP publication, Rome, 37-69.

Fournier, R.O., and Potter, R.W. II, 1982: A revised and expanded silica (quartz) geothermometer. *Geoth. Res. Council Bull., 11-10*, 3-12.

Fournier, R.O., and Rowe, J.J., 1966: Estimation of underground temperatures from the silica contents of water from hot springs and wet steam wells. *Am. J. Sci., 264,* 685-697.

Fournier, R.O., and Truesdell, A.H., 1973: An empirical Na-K-Ca geothermometer for natural waters. *Geochim. Cosmochim. Acta*, *37*, 1255-1275.

Friedman, I., 1953: Deuterium content of natural water and other substances. *Geochim. Cosmochim. Acta, 4*, 89-103.

Giggenbach, W.F., 1988: Geothermal solute equilibria. Derivation of Na-K-Mg-Ca geoindicators. *Geochim. Cosmochim. Acta, 52,* 2749-2765.

Giggenbach, W.F., 1991: Chemical techniques in geothermal exploration. In: D'Amore, F. (coordinator), *Applications of geochemistry in geothermal reservoir development.* UNITAR/UNDP publication, Rome, 119-142.

Gíslason, G., Ngobi, G., Isabirye, E., and Tumwebaze, S. 1994: *An Inventory of three Geothermal Areas in West and Southwest Uganda.* Prepared by the United Nations for a Project of the UNDP.

Gíslason, S.R., Heaney, P.J., Oelkers, E.H. and Schott, J., 1997: Kinetic and thermodynamic properties of moganite, a novel silica polymorph. *Geochim. Cosmochim. Acta, 61,* 1193-1204.

McNitt. J.R., 1982: The geothermal potential of East Africa. *Proceedings of the Regional Seminar on Geothermal Energy in Eastern and Southern Africa, Nairobi, Kenya*, 3-8.

Ministry of Finance, 2006: Budget 2006/2007. Ministry of Finance and Economic Development, Uganda, web page: *www.finance.go.ug.*

Morley, C.K., and Westcott, W.A., 1999: Sedimentary environments and geometry of sedimentary bodies determined from subsurface studies in East Africa. In: Morley, C.K. (ed.), *Geoscience of rift systems – evolution of East Africa.* AAPG Studies in Geology, 44, 211-231.

Reed, M.H., and Spycher, N.F., 1984: Calculation of pH and mineral equilibria in hydrothermal water with applications to geothermometry and studies of boiling and dilution. *Geochim. Cosmochim. Acta, 48*, 1479-1490.

Reed, M.H., and Spycher, N.F., 1989: *SOLVEQ: A computer program for computing aqueous-mineral-gas equilibria. A manual.* Department of Geological Sciences, University of Oregon, Eugene, Oregon 37 pp.

Sharma D.V 1971: *Report on the preliminary survey of thermal anomalies of Western Uganda for the possible development of geothermal energy*. Geological Survey and Mines Department, Uganda, unpubl. report DVS/3, 23 pp.

Stanley, H.M., 1890: *In darkest Africa.* New York, C. Scribner's Sons 2 V.; V.1, 547 pp., front., 73 illus., map; V.2, 540 p., front., 72 illus., maps.

Truesdell, A.H., 1976: Summary of section III - geochemical techniques in exploration. *Proceedings of the 2^{nd} U.N. Symposium on the Development and Use of Geothermal Resources, San Francisco, 1,* liii-lxxix.

Truesdell, A.H., and Fournier, R.O., 1977: Procedure for estimating the temperature of a hot water component in a mixed water using a plot of dissolved silica vs. enthalpy. *U.S. Geol. Survey J. Res., 5,* 49-52.

APPENDIX I: Example of sampling field record card

ÍSOR

Sample No. ______

Date/Time ______

Site/Site classification ______

Location ______

Sampled by ______

Project No./Supervisor ______

Coordinates ______

Site Description ______

RECORDS DURING SAMPLING

Depth (m) ______

Temperature °C ______

Flow/Estimated flow (kg/s) ______

Pressure (Ps) ______

Conductivity (μS/cm)/°C ______

Wellhead Pressure (Po) ______

Enthalpy (kJ/kg) ______

Discharge (kg/sec) ______

pH/°C ______

O_2 ______

H_2S ______

Notes ______

SUBSAMPLES (NO.)

Ru ______

Rd ______

Ra ______

Fu ______

Fa ______

Fp ______

Trace elements ______

Isotopes ______

SAMPLE HANDLING

Filters	0,45	0,20
not known	☐	☐
steel/acetate	☐	☐
PTFE/acetate	☐	☐
PTFE/nitrate	☐	☐
glass	☐	☐
plastic	☐	☐

Tariff 45	010	020	030	040	050	170	190	191	200	201				
Number														

APPENDIX II: Preservation methods for geothermal samples

Type	Method	Purpose	Used for
Physical	Filtration	Prevent interaction with suspended matter	Anions, cations
	Freezing	Prevent biological activity	Nutrients
	Airtight container	Prevent interaction with atmospheric air	Volatiles
	On-site analysis	Prevent reactions of reactive constituents	Reactive constituents
Chemical	Base addition	Absorption of acid gases	CO_2, H_2S in steam, $\delta^{34}S$ in H_2S in vapour
	Acidification	Prevent adsorption on walls of containers	Cations
	Precipitation	Prevent a constituent from reaction to change the concentration of another	Sulphide to preserve sulphate
	Sterilization	Prevent biological activity, using HgCl or formaldehyde	$\delta^{34}S$ and $\delta^{18}O$ in SO_4, prevents biological oxidation of sulphide
	Dilution	Prevent polymerization and precipitation	Silica
	Redox	To change oxidation state of a volatile constituent to make it less volatile	Hg
	Ion exchange	Concentrate and further prevent adsorption on walls of container of trace constituents	Trace cations
	Extraction	Concentrate and further prevent adsorption on walls of container of trace constituents	Trace cations

APPENDIX III: A set up of sample collection from a spring